

Microstructural and mechanical characterization of pearlitic steel after high intensity laser peening and shot peening

Nicholas Brooks, Majid Vaseghi, Lloyd Hackel, Keivan Davami

PII: S2213-8463(23)00211-0

DOI: <https://doi.org/10.1016/j.mfglet.2023.09.004>

Reference: MFGLT 776



To appear in: *Manufacturing Letters*

Received Date: 29 June 2023

Revised Date: 28 August 2023

Accepted Date: 15 September 2023

Please cite this article as: N. Brooks, M. Vaseghi, L. Hackel, K. Davami, Microstructural and mechanical characterization of pearlitic steel after high intensity laser peening and shot peening, *Manufacturing Letters* (2023), doi: <https://doi.org/10.1016/j.mfglet.2023.09.004>

This is a PDF file of an article that has undergone enhancements after acceptance, such as the addition of a cover page and metadata, and formatting for readability, but it is not yet the definitive version of record. This version will undergo additional copyediting, typesetting and review before it is published in its final form, but we are providing this version to give early visibility of the article. Please note that, during the production process, errors may be discovered which could affect the content, and all legal disclaimers that apply to the journal pertain.

Microstructural and mechanical characterization of pearlitic steel after high intensity laser peening and shot peening

Nicholas Brooks¹, Majid Vaseghi¹, Lloyd Hackel², Keivan Davami^{1*}

¹Department of Mechanical Engineering, University of Alabama, Tuscaloosa, AL, 35487, USA

²Curtiss Wright Surface Technologies, Metal Improvement Company, Livermore, CA, 94551, USA

*Corresponding Author: Keivan Davami (kdavami@eng.ua.edu)

Abstract

This study investigated the microstructural/mechanical properties of annealed 4340 pearlitic steel after shot peening (SP) and high intensity laser peening (LP). SP at 0.012-0.016A resulted in fragmentation of the pearlite colonies $\sim 1-2\mu\text{m}$ from the treated surface and sub-surface cracking as well as significant distortion of pearlite colonies $\sim 30\mu\text{m}$ from the treated surface. LP at a pulse energy of 19J with a pulse full-width half height of 27ns and a square spot size of $3\times 3\text{mm}^2$ resulted in an intense irradiance on the metal surface of 8GW/cm^2 . During this process a thin, micrometer-range layer of surface material is ablated which generates and heats a plasma plume in less than 1ns to a temperature in the range of 15,000K. A recast layer $\sim 5-10\mu\text{m}$ in thickness from the treated surface with significant porosity was observed in the LPed specimen. The highest average microhardness ($266\pm 9\text{HV}$) was observed in the SPed specimen $\sim 63\mu\text{m}$ from the treated surface, however the hardness quickly returned to the baseline hardness (218HV) $\sim 250-500\mu\text{m}$ from the treated surface. In the LPed specimen, the averaged microhardness values exceeded the baseline hardness up to a depth of $\sim 1500-2000\mu\text{m}$ with an average microhardness of $237\pm 4\text{HV}$ from $\sim 60-2500\mu\text{m}$ from the treated surface. It is shown that LP not only improves the sub-surface microhardness of the 4340 pearlitic steel up to greater depths than SP, but that it also preserves the pearlitic microstructure near the treated surface.

Keywords: Laser peening; Shot peening; Pearlitic steel; Mechanical characterization; Microstructural characterization

1. Introduction

Surface engineering techniques such as laser peening (LP) and shot peening (SP) are commonly used to enhance the surface and sub-surface mechanical properties of metals through the introduction of compressive residual stresses (CRSs) [1,2,3]. The introduction of CRSs and severe plastic deformation (SPD) coupled with high dislocation density provides substantial increases in strength against surface related failures such as fatigue and corrosion. It has been reported that LP can introduce CRSs to much greater depths in materials than SP which results in increased beneficial effects in LPed materials up to greater depths from the treated surface [4,5,6].

Surface enhancement techniques such as SP and LP have been investigated fairly extensively for 4340 steel [7,8,9,10], however, all of these studies have been performed on 4340 steel in its hardened (martensitic) state. These techniques are typically employed on metals after homogenization and heat treatment but they can also be employed on materials in their annealed conditions [11,12]. Previous studies involving SPD of ferrite-pearlite steels have shown that SPD can severely alter the pearlite colonies within ferrite-pearlite steels [11,13,14]. This has been shown to result in distortion and fragmentation of cementite within pearlite colonies near the surface of materials which can accelerate crack initiation and propagation due to the fracture characteristics of cementite platelets [15,16,17].

The novelty of this work lies in its investigation and comparison between the effects of high intensity LP and SP on the microstructural/mechanical properties of annealed 4340 steel which exhibits a primarily pearlitic microstructure. Distortion and fragmentation of the pearlite colonies after SP are shown to have assisted in the initiation and propagation of sub-surface cracks. The preservation of the pearlitic microstructure along with the high depth of

increased microhardness observed in the LPed specimen indicates that LP is more effective than SP for treating annealed 4340 steel.

2. Experimental Procedure

4340 steel with the chemical composition (wt.%): Ni-1.8, Cr-0.80, Mn-0.70, C-0.40, Mo-0.25, Fe-balance, is evaluated here. Specimens were fully annealed by heating at 800°C and then furnace cooled for 3.75hrs to 700°C [18]. SPed specimens were treated with cast steel shots conforming to AE AMS 2431/1 type ASR 330 cast steel shot standard. Full coverage treatment was performed on the specimens according to the SAE J2277 standard at an intensity between 0.012-0.016A. LPed specimens were peened with a solid-state laser operating at 19J with a pulse full-width half height of 27ns. A square spot size (3x3mm²) was used to cover the peened surface and 3 layers of peening were applied without an ablative overlay with a 33% overlap in both longitudinal and transverse directions. The irradiance on the metal surface, as calculated from the process parameters listed above, was 8GW/cm².

After treatment, specimens were mounted cross-sectionally, ground with 240-4000 grit SiC pads, and then polished with 9-1µm diamond suspensions and 0.05µm colloidal silica. A microhardness tester (Clemex MMT-X7B) was used to obtain hardness versus depth profiles. Vickers microhardness tests were performed with a diamond pyramid indenter at an applied load of ~5N (500gf) with a dwell time of 10s. A total of 136 indents were performed on each of the specimens ~60µm from the treated surfaces. Indents were separated by 150µm, and 8 indents were obtained at each depth up to ~2500µm from the treated surface. Specimens were then etched with Alder's etchant for 2-6s and imaged with an optical microscope (KEYENCE VHX-7000) and a scanning electron microscope (SEM) (Apreo 2, Thermo Fisher Scientific).

3. Results and Discussion

3.1. Microstructural Characterization

Images of the cross-sectioned un-treated, LPed, and SPed specimens showing the etched microstructures near the treated surface are included in Figs. 1(a-c). The annealed microstructure is composed of ferrite grains, which appear as white, and pearlite colonies which appear tan/brown. A distribution of ferrite and pearlite with a higher volume fraction of pearlite can be observed in all specimens.

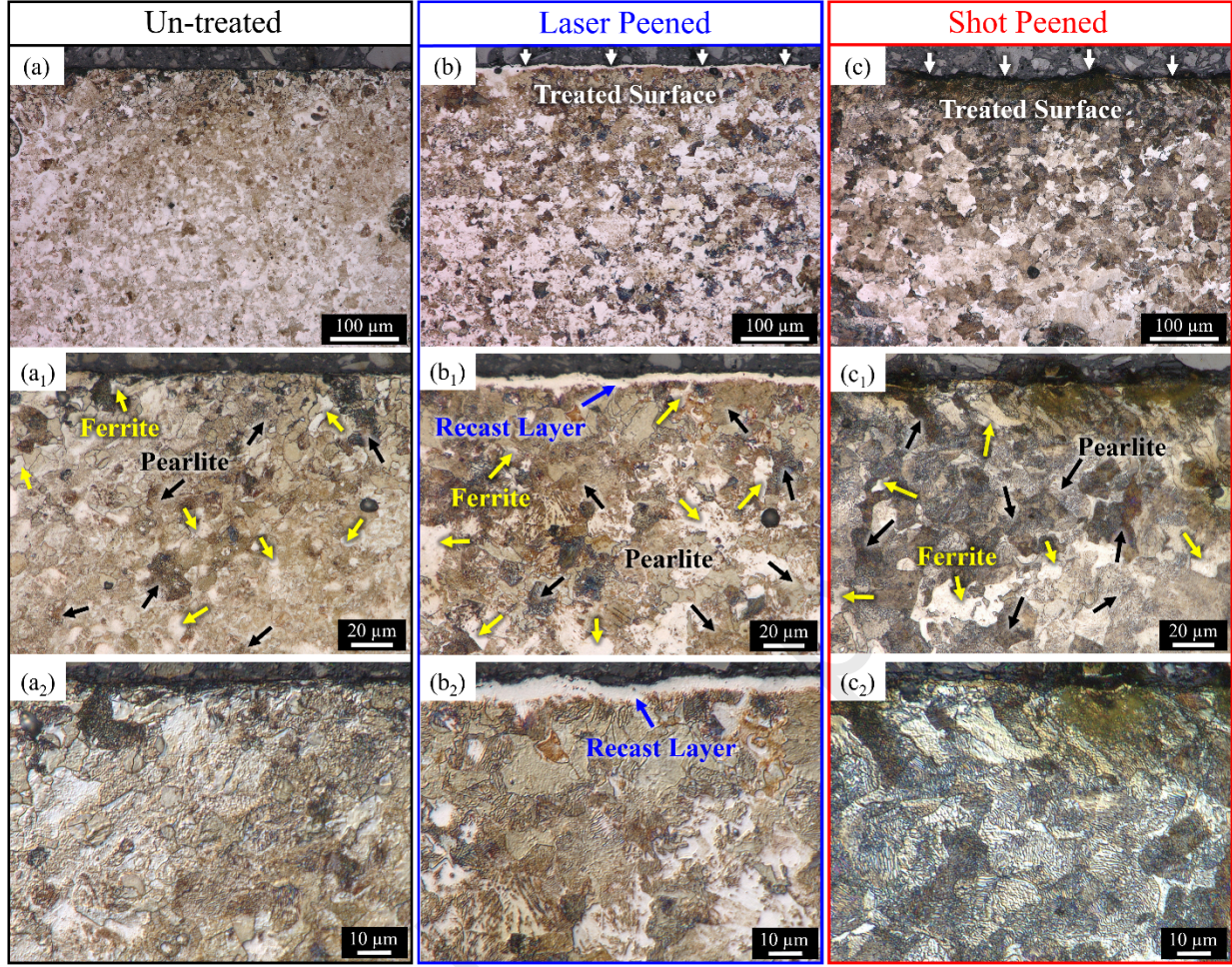


Fig. 1. Microstructures of the (a) un-treated, (b) LPed, and (c) SPed specimens.

The size and distribution of ferrite and pearlite remains consistent between the three specimens as expected, however there are some noticeable differences in the microstructure near the treated surfaces in the LPed and SPed specimens which can be seen by comparing Fig. 1(a₂) to Figs. 1(b₂) and 1(c₂). The most prominent feature present in the LPed specimen is the non-uniform recast layer which extends \sim 5-10 μ m from the treated surface (Fig. 1(b₂)). The existence of this recast layer is common in metals which have been LPed without an ablative overlay [19,20,21]. During LP without an ablative overlay, material at the surface melts and resolidifies. The recast layer tends to be very brittle due to the tensile stresses and the oxide film that are generated during resolidification and it often contains pores which result from the material resolidifying [19,21]. The microstructure of the SPed specimen appears to exhibit some distortion near the treated surface up to a depth of \sim 30 μ m from the surface (Fig. 1(c₂)).

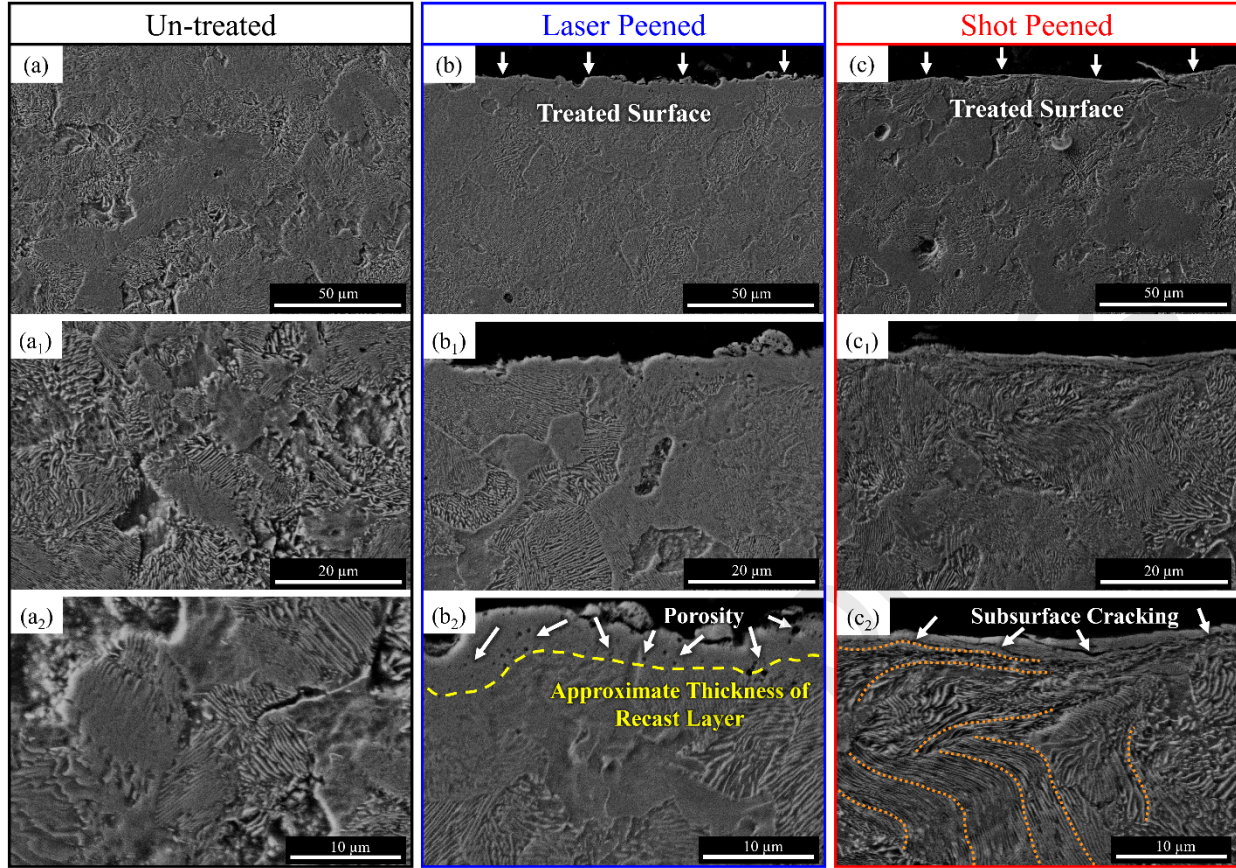


Fig. 2. Micrographs of the (a) un-treated, (b) LPed, and (c) SPed specimens.

The SEM provides improved spatial resolution of the microstructure of the annealed 4340 steel. Micrographs of the specimens are presented in Figs. 2(a-c). Sub-surface cracking extending $\sim 1-2\mu\text{m}$ and significant distortion of pearlite colonies up to $\sim 30\mu\text{m}$ from the treated surface can be observed in the SPed specimen (Fig. 2(c₂)). Orange dashed lines show the direction or distortion of the pearlite colonies near the SPed surface. This distortion of pearlite colonies has also been reported by others in pearlitic steels subjected to SPD [22,23,24]. In a study by Ivanisenko et al. [24], high pressure torsional tests were performed to investigate distortion of pearlite colonies under different shear strains. They found that the orientation of the pearlite colonies with respect to the applied shear strain greatly affected the distortion of cementite platelets within the pearlite colonies. It was also found that at high enough shear strain, the cementite platelets were no longer observed within the microstructure because they had dissolved into the ferrite matrix. In another study by Languillaume et al. [25] on cold drawn pearlitic steel it was concluded that SPD, which involves thinning of the cementite platelets and the generation of slip steps, caused the free energy of the cementite to increase. This increase in free energy made it unstable causing dissolution of the cementite into the supersaturated solid solution of C in ferrite. This finding was also corroborated by Korznikov et al. [26] in a study on high torsion straining of Fe-1.2C steel where they observed complete dissolution of the cementite phase following SPD.

Due to the brittle nature of the sub-surface cracks observed in the SPed specimen in Fig. 2(c₂) it was hypothesized that the cementite $\sim 1-2\mu\text{m}$ from the treated surface had not been dissolved into the ferrite matrix, but rather had been highly distorted and even fragmented. To investigate this further, higher magnification SEM images of the SPed and LPed surfaces have been performed (Figs. 3(a-b)).

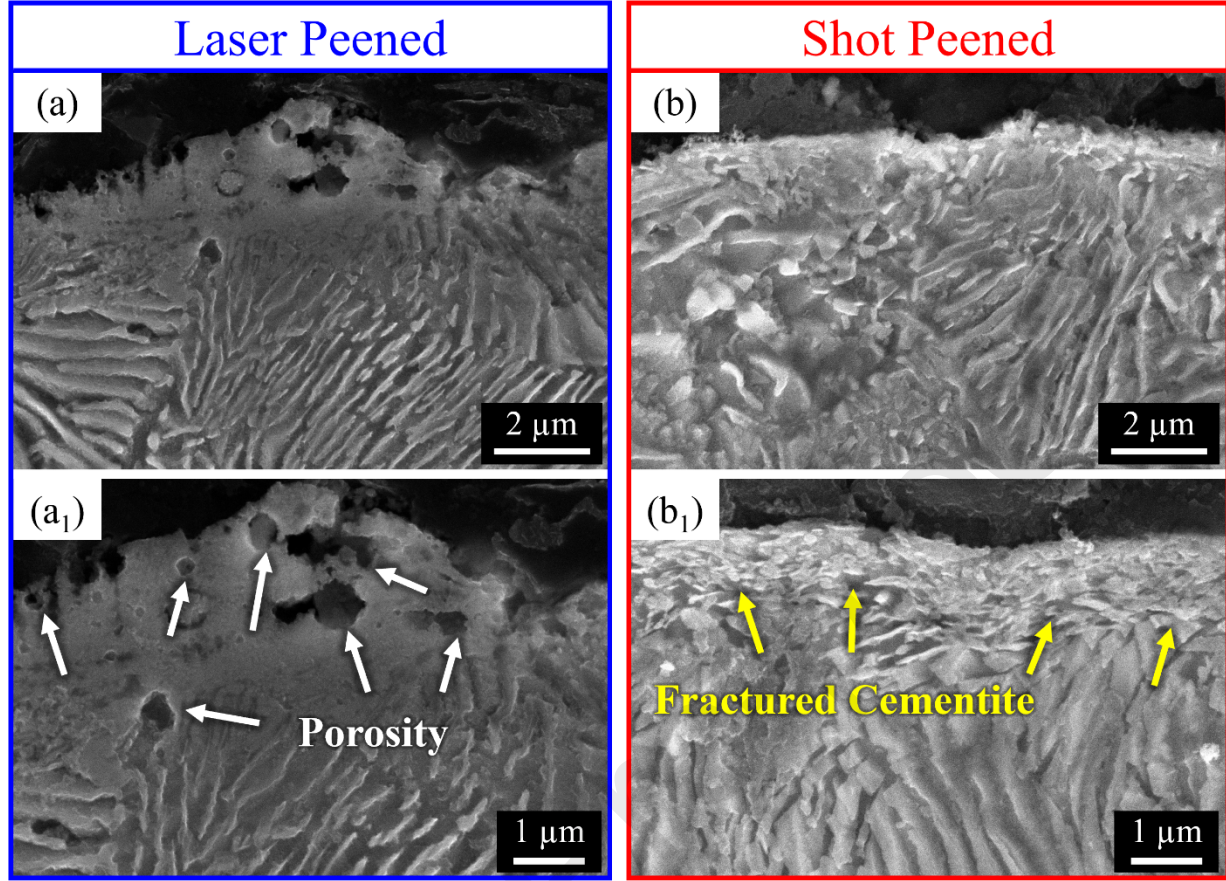


Fig. 3. Micrographs of the (a) LPed and (b) SPed specimens.

Figs. 3(a-a₁) show higher magnification images of the porous inner architecture observed in the LPed specimen within the recast layer, while Figs. 3(b-b₁) show the morphology of the cementite near the SPed surface. Here it can be seen that the region \sim 1-2 μ m from the treated surface contains highly distorted and fragmented cementite platelets. This phenomenon was also observed by Tung et al. [27] in Fe-0.74C steel after SPD induced by rolling contact fatigue where fragmentation of cementite platelets within pearlite was also realized up to a depth of \sim 2 μ m. It has been reported that the fracture mechanism of pearlite in 4340 steel is characterized by cracks running normal to pearlitic colonies (in between cementite platelets) [15]. This process occurs in pearlite colonies under the combined effects of applied stress tensile stress and shearing of the ferrite lamellae [16] which results in the separation of adjacent cementite platelets leading to microcracking. This observation accounts for the brittle nature of the cracks which were observed near the treated surface in the SPed specimen.

3.2. Microhardness

Microhardness contour plots obtained from the treated surfaces of each of the 4340 specimens are included in Figs. 4(a-c). The average microhardness in the SPed specimen \sim 63 μ m from the treated surface was measured to be 266 ± 9 HV. However, while this specimen exhibited the highest hardness near the surface, the increase in microhardness quickly dissipated \sim 250-500 μ m beneath the surface (Fig. 4(c)). In the LPed specimen, microhardness values exceeded the average baseline hardness (\sim 218 HV) up to \sim 1500-2500 μ m from the surface with an average measured microhardness of 237 ± 4 HV from the region \sim 60-2500 μ m from the treated surface (Fig. 4(b)). The increased depth of microhardness improvement is attributed to the increased depth of CRSs induced via LP as compared to SP [1,2,4].

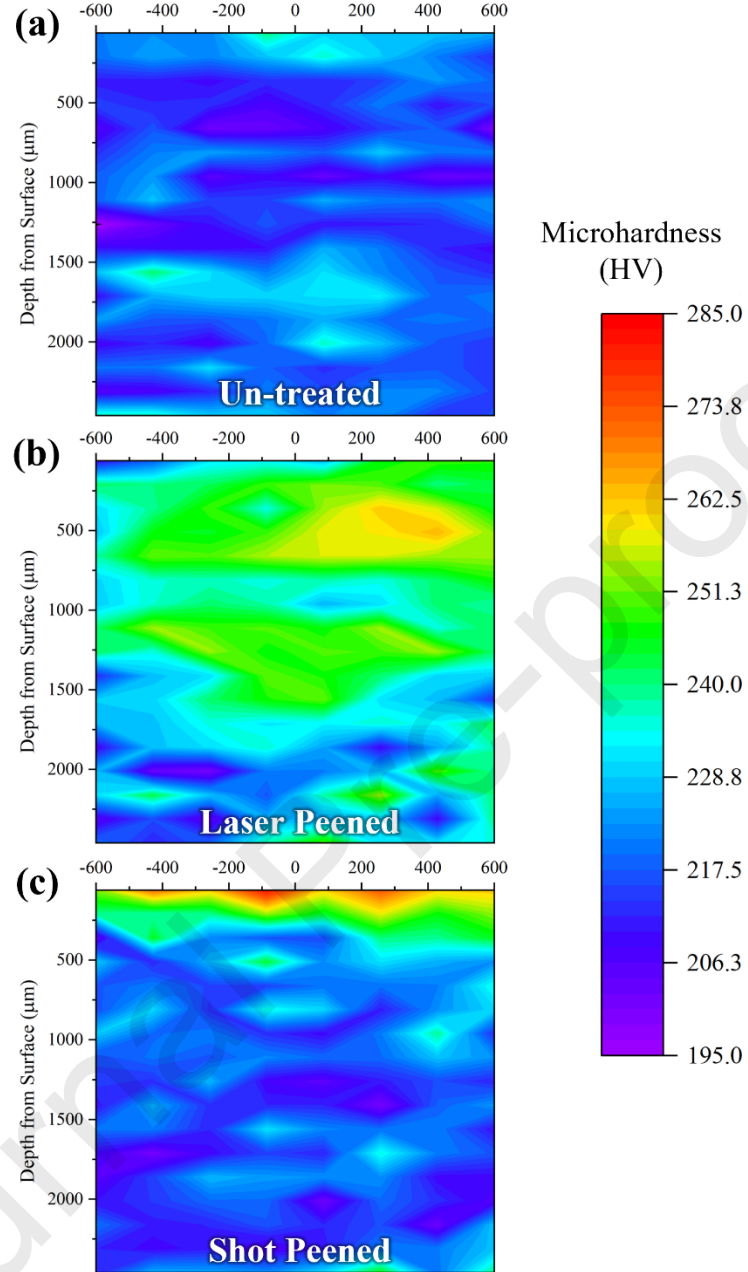


Fig. 4. Microhardness contour plots from the treated surface of the (a) un-treated, (b) LPed, and (c) SPed specimens.

These contour plots highlight the difference in the depth and uniformity of microhardness improvements between the SPed and LPed specimens. Comparing the results, it can be observed that the LPed specimen obtained a relatively uniform increase in hardness up to a much greater depth from the treated surface than the SPed specimen. These findings are consistent with previous studies which have shown the LP not only induces CRSs deeper into the material than SP, but that it also increases the hardness up to greater depths from the treated surface [1,2,4,6].

4. Conclusions

The influence of LP and SP on the microstructural/mechanical properties of annealed 4340 steel were investigated,

and the following conclusions were drawn.

1. The severe plastic deformation imparted by SP caused distortion and fragmentation of the cementite platelets within the pearlite colonies near the treated surface.
2. Sub-surface cracks were observed near the treated surface of the SPed specimens, while porosity was observed within the recast layer of the LPed specimen.
3. The sub-surface cracking observed in the SPed specimen is attributed to the distortion and fragmentation of cementite platelets.
4. The highest average microhardness (266 ± 9 HV) was observed in the SPed specimen at a depth of $\sim 62 \mu\text{m}$ from the surface. In the LPed specimen hardness improvements were observed up to ~ 1500 - $2000 \mu\text{m}$ with an average measured microhardness of 237 ± 4 HV from the region ~ 60 - $2500 \mu\text{m}$ from the treated surface.

Acknowledgment

This work was supported by the NSF, CMMI, Advanced Manufacturing Program (Award No.2029059).

References

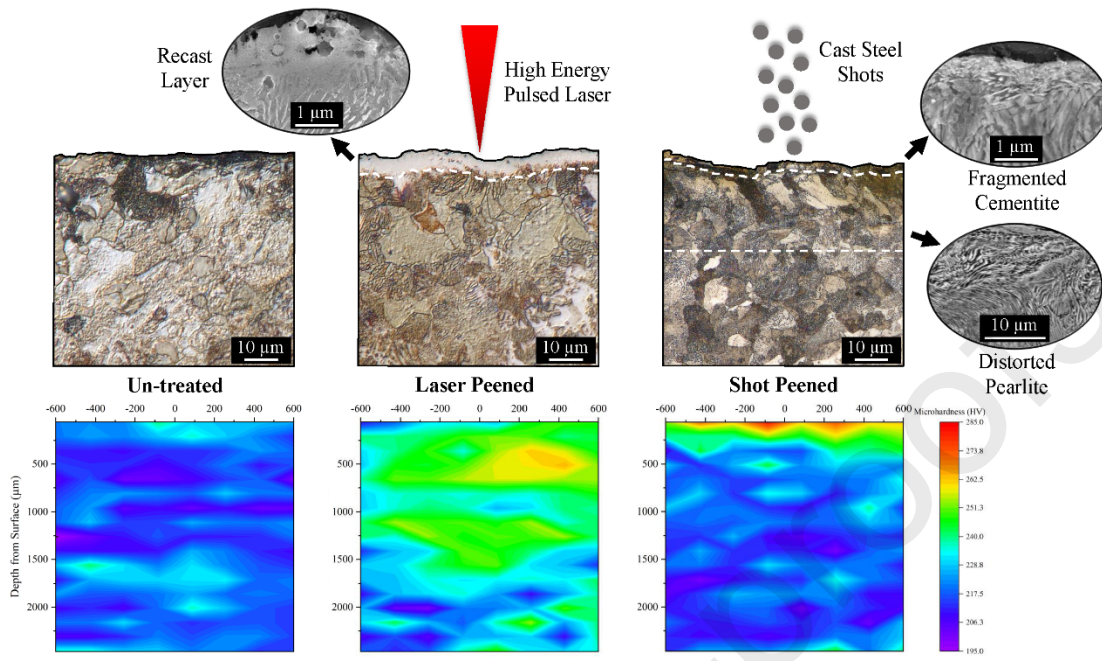
- [1] [Y. K. Gao, Mater. Sci. and Eng.: A. 528 \(2011\) 3823–3828.](#)
- [2] [A. Gujba, M. Medraj, Materials. 7 \(2014\) 7925–7974.](#)
- [3] [H. Soyama, J. of Mater. Processing Tech. 269 \(2019\) 65–78.](#)
- [4] [B. K. Pant, et al., Int. J. of Fatigue. 93 \(2019\) 38–50.](#)
- [5] [H. Soyama, A.M. Korsunsky, J. of Mater. Processing Tech. 305 \(2022\) 117586.](#)
- [6] [M. Munther, et al., Eng. Res. Express. 2 \(2020\) 022001.](#)
- [7] [R. A. Everett, et al., NASA/TM-2001-210843 \(2001\).](#)
- [8] [V. Llaneza, F. J. Belzunce, Appl. Surf. Sci. 356 \(2015\) 475-485.](#)
- [9] [Í. Tomaz, et al., Matéria. 25 \(2020\).](#)
- [10] [R. Karimbaev, et al., Mater. Sci. and Eng.: A. 791 \(2020\) 139752.](#)
- [11] [Y. Wang, et al., Int. J. of Hydrogen Energy. 45 \(2020\) 7169–7184.](#)
- [12] [M. Chen, et al., Surf. and Coat. Tech. 359 \(2019\) 511–519.](#)
- [13] [B. Karlsson, G. Lindén, Mater. Sci. and Eng. 17 \(1975\) 209–219.](#)
- [14] [J. A. Muñoz, et al., Mater. Sci. and Eng.: A. 805 \(2021\) 140624.](#)
- [15] [J. K. Cuddy, M. N. Bassim, Mater. Sci. and Eng.: A. 125 \(1990\) 43–48.](#)
- [16] [Y. J. Park, I. M. Bernstein, Metallurgical Trans. A. 10 \(1979\) 1653–1664.](#)

- [17] [K. Mishra, et al., Mater. Charact. 167 \(2020\) 110487.](#)
- [18] ASM handbook. 4 (1991)
- [19] [A. S. Gill, et al., J. of Mater. Processing Tech. 225 \(2015\) 463–472.](#)
- [20] [J. Kaufman, et al., Corrosion Sci. 194 \(2022\) 109925.](#)
- [21] [A. Sharma, et al., Scripta Materialia. 202 \(2021\) 114012.](#)
- [22] [G. Langford, Metallurgical Trans. A. 8 \(1977\) 861–875.](#)
- [23] [J. G. Sevillano, Mater. Sci. and Eng. 21 \(1975\) 221–225.](#)
- [24] [Yu. Ivanisenko, et al., Acta Materialia. 51 \(2003\) 5555-5570.](#)
- [25] [J. Languillaume, et al., Acta Materialia. 45 \(1997\) 1201-1212.](#)
- [26] [A. V. Korznikov, et al., Nanostructured Mater. 4 \(1994\) 159-167.](#)
- [27] [P.-Y. Tung, et al., Acta Materialia. 216 \(2021\) 117144.](#)

Declaration of interests

- The authors declare that they have no known competing financial interests or personal relationships that could have appeared to influence the work reported in this paper.
- The authors declare the following financial interests/personal relationships which may be considered as potential competing interests:

Keivan Davami reports financial support was provided by National Science Foundation.



Highlights

- SP caused distortion and fragmentation of cementite platelets near the surface.
- LP without an ablative layer resulted in a recast layer \sim 5-10 μm thick.
- LP resulted in microhardness increases up to \sim 1500-2000 μm from the surface.
- SP resulted in sub-surface cracking near the surface.